Published in final edited form as:
J Pharm Sci. 2013 March ; 102(3): 892–903. doi:10.1002/jps.23387.

Characterization of Human Sclera Barrier Properties for Transscleral Delivery of Bevacizumab and Ranibizumab

He Wen, **Jinsong Hao**, and **S. Kevin Li**
Division of Pharmaceutical Sciences, James L. Winkle College of Pharmacy, University of Cincinnati, Cincinnati, Ohio 45267

Abstract

The objectives of this study were to (a) investigate transscleral permeation of antivascular endothelial growth factor drugs bevacizumab and ranibizumab and (b) examine the effects of molecular structures of macromolecules upon permeation across human sclera using bevacizumab, ranibizumab, fluorescein isothiocyanate (FITC)-labeled bovine serum albumin (FITC-BSA), FITC-labeled ficoll (FITC-ficoll), and FITC-labeled dextrans (FITC-dextrans) *in vitro*. The hydrodynamic radii of the macromolecules were measured using dynamic light scattering, their partition coefficients to sclera were determined in uptake experiments, and their permeability coefficients and transport lag times across sclera were evaluated in transport experiments of side-by-side diffusion cells. Macromolecules showed relatively low partition coefficients to sclera. The partition coefficient of FITC-BSA was found to be related to its concentration in the equilibration solution, whereas for other macromolecules, no specific concentration dependency was observed. The macromolecules displayed relatively low permeability coefficients and long transport lag times because of their molecular sizes and hindered diffusion. Bevacizumab, ranibizumab, and FITC-BSA exhibited lower transscleral permeability and longer transport lag times than FITC-dextrans and FITC-ficoll of comparable molecular weights possibly because of the flexible structures of the polysaccharides. Thus, the polysaccharides may not be good surrogate permeants to model transscleral transport of therapeutic proteins in transscleral delivery studies.

Keywords

bevacizumab; ranibizumab; dextran; macromolecular drug delivery; protein delivery; passive diffusion/transport; permeability; ocular drug delivery; transscleral delivery; human sclera

INTRODUCTION

Neovascular eye diseases such as wet age-related macular degeneration and proliferative diabetic retinopathy are among the leading causes of visual impairment in older people in developed countries.[1–3] Vascular endothelial growth factor (VEGF) is believed to play an important role in the pathology of these diseases, which is related to abnormal neovascularization and the increase of vascular membrane permeability and fragility[4–6] Therapies utilizing anti-VEGF agents have been studied and shown as promising approaches for treating neovascular eye diseases.[7,8] Bevacizumab (Avastin®) is a recombinant humanized monoclonal immunoglobulin G1 antibody inhibiting all active isoforms of VEGF-A. It is primarily approved by US Food and Drug Administration (FDA) as an anticancer agent. Intravitreal administration of bevacizumab is used off-label in the

Correspondence to: He Wen (Telephone: +513-558-0398; Fax: +513-558-4372; wenhe@mail.uc.edu).

treatment of neovascular ocular diseases. Ranibizumab (Lucentis®) is a monoclonal Fab fragment of bevacizumab. The intravitreal injection of ranibizumab has been approved by FDA for the treatment of neovascular (wet) age-related macular degeneration and diabetic retinopathy following retinal vein occlusion. Intravitreal administrations of both bevacizumab and ranibizumab have demonstrated benefits to patients when they are used in neovascular ocular disease treatments in clinical studies.[9–11]

Because of the chronic nature of these neovascular ocular diseases, multiple intravitreal injections are usually required in the treatments, and adverse effects such as vitreous hemorrhage, ocular inflammation, retinal detachment, and cataract have been reported to be associated with repeated intravitreal injections.[12–14] It is desirable to develop a safer and more effective drug delivery system for treating neovascular eye diseases than conventional intravitreal injections. Human sclera has a large and accessible surface area of approximately 16.3 cm^2, which constitutes about 95% of the total surface area of the eye globe.[15,16] Sclera is also a highly permeable tissue. Previous studies have shown that sclera is permeable to large molecules, for example, therapeutic proteins, with molecular weights up to 150 kDa.[17–21] Therefore, transscleral delivery, taking advantages of the large surface area and high permeability of sclera, could offer an alternative approach to deliver anti-VEGF drugs to the posterior segment of the eye.

Dextrans are polysaccharides with linear structures and behave like random coils. Ficolls are cross-linked polymers of sucrose and epichlorohydrin with relatively spherical shapes. With the neutral molecular charge and commercial availability of a wide range of molecular weights, dextrans and ficolls are frequently employed as molecular probes to study the permeability of membranes to biological macromolecules such as proteins. The comparison of scleral uptake and transscleral transport behaviors of the polysaccharides with those of anti-VEGF proteins is expected to provide insight into the effects of influencing factors such as molecular charge, size, and shape on the transscleral delivery of bevacizumab and ranibizumab.

The objectives of the present study were to (a) determine the partition coefficients of bevacizumab and ranibizumab to human sclera, (b) determine the permeability coefficients and lag times of bevacizumab and ranibizumab transporting across human sclera, and (c) examine whether the transscleral transport of anti-VEGF proteins can be approximated by polysaccharides (e.g., dextrans and ficolls) of equivalent molecular weights. The partition and permeation data would be useful in the evaluation of transscleral delivery of bevacizumab and ranibizumab and in the development of drug delivery systems for these anti-VEGF proteins utilizing the transscleral route.

MATERIALS AND METHODS

Materials

Phosphate-buffered saline (PBS, pH 7.4; consisting of 0.01 M phosphate buffer, 0.0027 M potassium chloride, and 0.137 M sodium chloride) was prepared by dissolving PBS tablets (Sigma–Aldrich, St. Louis, Missouri) in distilled, deionized water. Gentamicin sulfate (Sigma–Aldrich) was added in PBS to a final concentration of 50 μg/mL as the preservative. Bevacizumab (Avastin®, 100 mg in 4 mL) and ranibizumab (Lucentis®, 2 mg in 0.2 mL) were from Genentech, Inc. (Oceanside, California). Bovine serum albumin (BSA) and fluorescein isothiocyanate (FITC)-labeled BSA (FITC-BSA) (≥ 7 mol FITC per mol albumin) were purchased from Sigma– Aldrich. FITC-labeled ficoll (FITC-ficoll) with average molecular weight of 70 kDa was purchased from Sigma–Aldrich. FITC-labeled dextrans (FITC-dextran) with average molecular weights of 20, 40, and 150 kDa (0.003–0.020 mol FITC per mol glucose) were purchased from Sigma–Aldrich. Dextran standards

with average molecular weights of 47 and 144 kDa were purchased from American Polymer Standards Corporation (Mentor, Ohio). Millipore filters with 0.45 μm pore size (Zymark®) were purchased from Millipore Corporation (Bedford, Massachusetts). MCE membrane filters with 0.22 μm pore size were purchased from Fisher Scientific (Rochester, New York).

Human cadaver eyes were obtained from the National Disease Research Interchange (NDRI, Philadelphia, Pennsylvania) and Moran Eye Center at the University of Utah (Salt Lake City, Utah). Human donors included both men and women, from 21 to 80 years of age, without any known eye diseases. The tissues were stored in moist chambers at 4°C before the experiments and the equatorial parts of the sclera from the whole poles were used in the study. The use of human tissues was approved by the Institutional Review Board at the University of Cincinnati (Cincinnati, Ohio).

Permeant Size Measurement

The average hydrodynamic radii of bevacizumab, ranibizumab, BSA, FITC-BSA, FITC-ficoll 70 kDa, FITC-dextran 20 kDa, FITC-dextran 40 kDa, and FITC-dextran 150 kDa were determined by dynamic light scattering using Malvern Zetasizer® Nano ZS at 25°C and analyzed using Dispersion Technology Software (Malvern Instruments Ltd., Malvern, Worcestershire, United Kingdom). Bevacizumab and ranibizumab solutions were prepared by diluting Avastin® and Lucentis® (Genentech, Inc.) with PBS and then filtered using 0.45 μm filters. BSA and FITC-BSA solutions were prepared by dissolving BSA and FITC-BSA in PBS and then filtered using 0.45 μm filters. FITC-ficoll 70 kDa and FITC-dextran 20, 40, and 150 kDa solutions were prepared as follows. Because the unlabeled polymers could interfere with the size measurements of the FITC-labeled polymers in dynamic light scattering study, FITC-ficoll and FITC-dextrans were first fractionated using high-performance liquid chromatography (HPLC) (see the section *HPLC Assay*) to remove the unlabeled polymers. The fractionated FITC-labeled polymer solution was collected, dried overnight, and reconstituted in PBS. FITC-dextran 40 kDa solution was filtered using 0.45 μm filter. FITC-ficoll 70 kDa, FITC-dextrans 20 and 150 kDa solutions were filtered using 0.22 μm filters because of the appearance of dynamic light scattering peaks in the 0.2–0.4 μm range in the samples. Gold nanoparticles (RM 8011; National Institute of Standards and Technology (NIST), Gaithersburg, Maryland) were used as the standard to qualify the instrument. Dextran standards 47 and 144 kDa were the other controls. The sizes of BSA and FITC-BSA were compared to examine the possible influence of the FITC label on the hydrodynamic size measurements.

Uptake Experiment

Before the uptake experiments, the adhering tissues on the sclera were carefully removed. The sclera was cut into a square-shaped sample and equilibrated in PBS in a vial at room temperature. After equilibration, the sclera was removed from the vial and blotted with Kimwipes® (Kimberly-Clark Professional, Roswell, Georgia) to remove the solution on the surface, and the wet weight of the hydrated sclera was quickly determined. The sclera was then dried at room temperature overnight until a constant dry weight was obtained. The average weight of the wet sclera was 0.059 g (ranging from 0.034 to 0.096 g), and the water content of the sclera was about 75% of the sclera wet weight in the present study, consistent with the value obtained in a previous study.[22]

Equilibration solutions were prepared by diluting Avastin® and Lucentis® (Genentech, Inc.) with PBS or dissolving FITC-BSA, FITC-ficoll 70 kDa, FITC-dextran 20 kDa, FITC-dextran 40 kDa, and FITC-dextran 150 kDa in PBS to a concentration of 1–12 mg/mL. The solutions were filtrated using 0.45 or 0.22 μm filters as described in the section *Permeant Size Measurement*. The dry sclera was allowed to equilibrate in the equilibration solution for

3 days at room temperature with occasional agitation. The 3-day equilibration time was selected based on a preliminary study showing no significant difference between the partition results with 3-day and 5-day equilibration. After equilibration, the sclera was removed from the equilibration solution, blotted with Kimwipes®, and placed in PBS in a vial for extraction at room temperature. After 48-h extraction, the sclera was removed from the vial and placed into another vial containing fresh PBS, and a second extraction step was performed. This extraction procedure was repeated on the same sclera until the amounts of permeant extracted into PBS were less than 10% of the amounts in the first extraction. The extraction solutions in the vials and the equilibration solutions were stored at 4°C before assay. All experiments were performed under light-shielding condition. Control uptake experiments were conducted in PBS in the absence of the permeants following the same procedure.

The partition coefficient (K_{sclera}) was defined as the ratio of the apparent concentration of the permeant in the sclera to the concentration of the permeant in the equilibration solution:

$$K_{\text{sclera}} = \frac{M_{\text{extraction}}/W_{\text{wet}}}{C_{\text{equilibration}}} \quad (1)$$

where $M_{\text{extraction}}$ is the total amount of permeant extracted from the sclera, W_{wet} is the wet weight of the sclera, and $C_{\text{equilibration}}$ is the concentration of permeant in the equilibration solution at the end of tissue equilibration. For the permeants with molecular charges that can be influenced by solution pH and ionic strength (i.e., the proteins), the partition coefficients describe permeant distribution between the sclera and the PBS equilibration solution (i.e., at physiological pH and ionic strength).

To validate the extraction method, the recovery of permeant extraction in the uptake experiments was examined. Briefly, 10-μL equilibration solution was pipetted onto the surface of dry sclera. After the complete uptake of the solution, the sclera was placed in PBS in a vial for extraction following the same method as described above. The percent of recovery was calculated by mass balance of the permeant and presented as the ratio of the total amount of permeant extracted from the sclera to the amount of permeant in the pipetted equilibration solution.

Transport Experiment

Transport experiments were conducted in side-by-side diffusion cells with an effective diffusion area of approximately 0.8 cm^2 under well-stirred conditions. The sclera was prepared by removing the adhering tissues and equilibrating it in PBS, as described in the section *Uptake Experiment*. The thickness of the hydrated sclera was measured using a micrometer (Mitutoyo, Kawasaki, Kanagawa, Japan). The sclera had thickness ranging from 0.6 to 1.0 mm in the present study. The hydrated sclera was mounted between two half-cells of the side-by-side diffusion cells with the episcleral side facing the donor chamber. The diffusion cells were then placed in a circulating water bath at 37 ± 1°C. Donor solutions were prepared by diluting Avastin® and Lucentis® (Genentech, Inc.) with PBS or dissolving FITC-BSA, FITC-ficoll 70 kDa, FITC-dextran 20 kDa, FITC-dextran 40 kDa, and FITC-dextran 150 kDa in PBS and filtering the solutions using 0.45 or 0.22 μm filters as described in the section *Uptake Experiment*. The donor concentrations during the experiments were measured and found to be 1.3 ± 0.1, 1.2 ± 0.5, 4.2 ± 0.2, 2.8 ± 0.3, 1.9 ± 0.3, 2.1 ± 0.1, and 2.1± 0.1 mg/mL for bevacizumab, ranibizumab, FITC-BSA, FITC-ficoll 70 kDa, FITC-dextran 20 kDa, FITC-dextran 40 kDa, and FITC-dextran 150 kDa, respectively. PBS was the receptor solution. The volumes of the donor and receptor solutions were 2.5 mL. The durations of the transport experiments were 48 h for ranibizumab and 96 h for the other permeants. These durations allowed the transport experiments to reach steady state. At

predetermined time points, 1-mL samples were withdrawn from the receptor chamber, and fresh PBS was added to the receptor chamber to maintain a constant volume of the receptor solution. At the same time, 5-μL samples of bevacizumab and ranibizumab or 10-μL samples of FITC-BSA, FITC-ficoll, and FITC-dextrans were withdrawn from the donor chamber. The donor solution was replaced with fresh donor solution every 16–48 h to maintain constant concentration in the donor chamber during the experiment. All experiments were conducted under light-shielding condition, and the samples were stored at 4°C before assay. The duration of the transport experiment was well within the length of human sclera tissue stability determined in a previous study (unpublished data).

The cumulative amount of the permeant transported across the sclera (Q) was plotted against time (t). The apparent flux of the permeant (J) was calculated from the least squares slope of the linear region in the Q versus t plot ($\Delta Q/\Delta t$) divided by the effective diffusion area (A). The transport lag time (t_{lag}) was calculated from the x-intercept of the linear regression line in the Q versus t plot. The apparent permeability coefficient (P) was calculated by dividing the flux by the concentration of the permeant in the donor (C_D):

$$J=\frac{1}{A}\frac{\Delta Q}{\Delta t} \quad (2)$$

$$P=\frac{1}{C_D A}\frac{\Delta Q}{\Delta t} \quad (3)$$

Solution Viscosity Measurement

To evaluate possible influence of solution viscosity on permeant transport, the viscosities of the donor solutions were determined. Solution viscosity was measured using an Ostwald dropping pipet (Fisher Scientific) at room temperature. Water viscosity was used as the reference in the viscosity calculation. Results from the measurements showed no significant difference (within 3%) between the viscosities of these solutions and water, indicating that the viscosity of the donor solution was not a major factor affecting transscleral transport in the present study.

Stability Study

The stability of bevacizumab and ranibizumab under storage at 4°C and room temperature was evaluated over a period of 2 weeks. Briefly, bevacizumab and ranibizumab solutions of 0.5 mg/mL were stored in a refrigerator at 4°C or placed on the bench at room temperature. At the end of each week, a 2-μL sample was withdrawn from each vial and the drug concentrations were analyzed and compared.

Enzyme-Linked Immunosorbent Assay

Bevacizumab and ranibizumab samples were analyzed by enzyme-linked immunosorbent assay (ELISA). Bevacizumab and ranibizumab samples were first diluted by 0.05% (w/v) BSA in PBS. 100 μL of each sample was then added into an antihuman IgG 96-well assay plate (BD Biosciences, San Jose, California). After 1-h incubation, the plate was washed three times with 0.02% Tween-20 (Sigma–Aldrich) in PBS. Subsequently, 100 μL biotinylated rhVEGF (R&D System, Minneapolis, Minnesota) diluted with 0.05% (w/v) BSA in PBS was added to each well and allowed to incubate for 1 h, followed by three washings with 0.05% Tween-20 (Sigma–Aldrich) in PBS. The wells were then incubated with 100 μL streptavidin–horseradish peroxidase (BD Biosciences) diluted 1:16,000 with 0.05% (w/v) BSA in PBS for 1 h and washed with 0.02% Tween-20 (Sigma–Aldrich) in

PBS three times. After that, 100 μL TMB substrate reagent (a mixture of hydrogen peroxide and 3,3′, 5,5′ tetramethylbenzidine in an organic solvent; BD Biosciences) was added to each well, and the reaction was allowed to carry out for 8 min and stopped with 50 μL 1 M H_3PO_4 (Fisher Scientific). The absorbance was determined immediately using a SpectraMax 250 (GMI, Inc., Ramsey, Minnesota) microplate reader at 450 nm, with the subtraction of the reference absorbance at 650 nm. All incubations were performed at room temperature and were protected from light. Samples were analyzed in duplicate, and a calibration curve of known concentrations of bevacizumab and/or ranibizumab in 0.05% (w/v) BSA in PBS prepared using fresh bevacizumab and ranibizumab was included in each individual assay. The detection limit of this assay was approximately 1 ng/mL.

HPLC Assay

The concentrations of FITC-BSA, FITC-ficoll, and FITC-dextrans were measured by HPLC. The HPLC system (Prominence; Shimadzu, Columbia, Maryland) consisted of CBM-20A system controller, LC-20AT solvent delivery unit, SIL-20A autosampler, and SPD-20A UV–Vis detector. Separation was performed using a size-exclusion column (TSKgel G4000PWxl, 7.8 mm × 300 mm; Tosoh Bioscience LLC, King of Prussia, Pennsylvania) at room temperature. Distilled, deionized water was used as the mobile phase and the flow rate was 0.5 mL/min. UV absorbance of the FITC-labeled permeants was measured at 494 nm. Calibration curves were established in the range of 8–200 μg/mL ($r^2 > 0.999$).

Statistical Analysis

The Student's *t*-test with one-tailed distribution was employed to evaluate the statistical differences in the experiments. Differences were considered to be significant at a level of $p < 0.05$. The means ± standard deviations of the data are presented.

Theory and Equations

The permeability of polar permeants across a porous membrane with uniform pores can be described by[23]:

$$P=\frac{\varepsilon HD}{\tau h} \quad (4)$$

where ε is the porosity and τ is the tortuosity of the membrane, H is the hindrance factor, D is the free aqueous diffusion coefficient of the permeant, and h is the thickness of the membrane. Assuming cylindrical pore geometry in the membrane and using the centerline approximation, the hindrance factor H for Brownian diffusion can be expressed by[24]:

$$H(\lambda)=\frac{6\pi(1-\lambda)^2}{K_t} \quad (5)$$

where λ is the ratio of permeant radius (r_s) to pore radius (R_p), and K_t is calculated by:

$$K_t=\frac{9}{4}\pi^2\sqrt{2}(1-\lambda)^{-5/2}\left[1+\sum_{n=1}^{2}a_n(1-\lambda)^n\right]+\sum_{n=0}^{4}a_{n+3}\lambda^n \quad (6)$$

where $a_1 = -1.217$, $a_2 = 1.534$, $a_3 = -22.51$, $a_4 = -5.612$, $a_5 = -0.3363$, $a_6 = -1.216$, and $a_7 = 1.647$. The hindrance factor describes the differential partitioning and diffusion of the permeants across the pores in the membrane due to permeant sizes. In Eq. 5, $(1 - \lambda)^2$ is the partition coefficient related to the steric exclusion of the permeant from the pores in bulk solution and $6\pi/K_t$ is related to the hydrodynamic factor of hindered diffusion in the pores.

With the hindered diffusion theory and the assumption that the permeants utilize a single transport pathway across the sclera, the effective pore size of the membrane can be estimated from the ratio of the permeability coefficients of the permeants obtained from the transport experiment using Eqs. 5–7.

$$\frac{P_i}{P_j}=\frac{H_i D_i}{H_j D_j} \quad (7)$$

where subscripts *i* and *j* represent permeants *i* and *j*, respectively. It should be noted that the effective pore size determined with Eq. 7 is an experimental factor describing the barrier properties of the sclera to the macromolecules for predicting transscleral permeation. The transport pathway in the sclera is not necessarily cylindrical pores, and other factors such as pore geometries are absorbed into the determined effective pore size. For a porous membrane with uniform pores, the transport lag time can be described by:

$$t_{\mathrm{lag}}=\frac{(\tau h)^2}{6HD} \quad (8)$$

RESULTS

Size Measurement

Table 1 summarizes the hydrodynamic radii of the permeants determined in the present study. For the anti-VEGF drugs, bevacizumab with the higher molecular weight displayed a larger hydrodynamic radius than ranibizumab. For the FITC-dextrans, the hydrodynamic radii increased in the order as their molecular weights. When the hydrodynamic radii of the proteins and polysaccharides were compared at similar molecular weights, the polysaccharides tended to have larger hydrodynamic radii than the globular proteins. The hydrodynamic radius of FITC-dextran 150 kDa was about 1.4 times larger than that of bevacizumab. FITC-dextran 40 kDa showed a 1.6 times larger hydrodynamic radius than ranibizumab. Even FITC-dextran 20 kDa exhibited larger hydrodynamic radius than ranibizumab. FITC-ficoll showed a 1.3 times larger hydrodynamic radius than FITC-BSA. The disparity in hydrodynamic radii between the polysaccharides and proteins is in agreement with that observed in a previous study.[25]

The hydrodynamic radius of BSA (4.8 ± 0.2 nm) in the present study is consistent with the literature value[26] and is believed to be the average value composed of both dimer and monomer.[27,28] In the comparison of the hydrodynamic radii of BSA and FITC-BSA, the hydrodynamic radii of BSA and its fluorescence-labeled counterpart were essentially the same, although FITC-BSA was slightly larger possibly because of the addition of fluorophores on FITC-BSA. This result indicates that the fluorescence labels on the macromolecules did not affect the size measurements. Moreover, the hydrodynamic radii of FITC-dextran 40 kDa and dextran standard 47 kDa (6.1 ± 0.1 nm) and those of FITC-dextran 150 kDa and dextran standard 144 kDa (10.0 ± 0.2 nm) were generally in agreement, which further validated the measurements.

Figure 1 is a plot of the relationship between the aqueous diffusion coefficients and the molecular weights of the permeants at 37°C in the present study. A general trend of decreasing diffusion coefficients with the increase in molecular weights for both proteins and polysaccharides was observed. The overall diffusion coefficients of proteins bevacizumab, ranibizumab, and FITC-BSA were higher than those of dextrans and ficoll as anticipated from the hydrodynamic size data above.

Uptake Study

The uptake of permeants to human sclera at different equilibrium concentrations of the permeants in the equilibration solutions showed two different patterns. The relationships between the partition coefficients and the equilibrium concentrations for two representative permeants FITC-BSA and FITC-dextran 150 kDa are presented in Figure 2. The partition coefficient of FITC-BSA was observed to be concentration dependent such that FITC-BSA at higher equilibrium concentrations exhibited lower partition coefficients to the sclera. On the contrary, no specific concentration dependency of partition coefficients was found for the other permeants; the partition coefficients of these permeants were essentially within the same range under the equilibrium concentration range studied and within the uncertainty of the data. Table 2 summarizes the uptake data in the present study. In general, the average partition coefficients of the macromolecules ranged from approximately 0.3 to 0.5. The overall partition coefficients of the studied macromolecules were approximately 2.4 times lower than the small hydrophilic molecules (with logarithm of octanol-PBS distribution coefficient, log $D_{oct} < 0$) in a previous study.[22]

In a separate study, the recovery of the extraction method was checked and found to be above 80% for all the permeants studied. In the control experiment of scleral uptake without the permeants, the result showed no detectable endogenous compounds from the sclera that significantly interfered with the assay of the equilibration solution during extraction.

Transport Study

Figure 3 presents the plots of cumulative amounts of permeants transported across the sclera versus time for the permeants. Permeant transport across the sclera was observed to approach steady state by the end of the experiments. Figure 4 shows the relationship between the permeability coefficients and the molecular weights of the permeants. A trend of decreasing permeability coefficients with increasing molecular weights was observed. This is consistent with the general relationship between molecular weight and permeant transport across a porous membrane.[18,19] Particularly, the permeability coefficients of the sclera for the macromolecules were at least 14 times smaller than that for the small hydrophilic molecules (log $D_{oct} < 0$) in a previous study[22] It should be noted that the permeability coefficients for bevacizumab and FITC-BSA in the present study ($2.9 \times 10^{-7} \pm 1.4 \times 10^{-7}$ and $9.0 \times 10^{-7} \pm 5.0 \times 10^{-7}$ cm/s, respectively) were lower than those presented in a previous study ($7.8 \times 10^{-7} \pm 0.8 \times 10^{-7}$ and $2.5 \times 10^{-6} \pm 0.6 \times 10^{-6}$ cm/s, respectively)[19] by a constant factor, that is, the absolute permeability coefficients were different in the present and previous studies but the ratios of bevacizumab to BSA permeability coefficients in both studies were essentially the same. This may be due to sclera-to-sclera variability from different sclera donors (e.g., different sclera thicknesses).

To examine the relationship between the permeability coefficients and molecular weights of the permeants, the permeability coefficients of the permeants were normalized by the free aqueous diffusion coefficients of the permeants and tissue thicknesses and plotted against their molecular weights (Fig. 5). These normalized permeability coefficients are directly proportional to the hindrance factors in Eq. 4. If there was no hindered diffusion in transscleral transport, the normalized permeability values of the macromolecules in the present study should be essentially the same as those of the small hydrophilic molecules (log $D_{oct} < 0$) in a previous study.[22] The results in the figure show that the normalized permeability coefficients of the macromolecules were lower than those of the small molecules, suggesting transport hindrance for the macromolecules. In addition, both dextrans and ficoll exhibited higher normalized permeability coefficients than bevacizumab, ranibizumab, and FITC-BSA ($p < 0.05$), indicating that the sclera was effectively more permeable to the polysaccharides than the rigid proteins of comparable molecular weights.

Ranibizumab, which has lower molecular weight of the two anti-VEGF proteins, displayed approximately two to three times higher normalized permeability coefficient than bevacizumab. On the contrary, the normalized permeability coefficients were essentially the same for the FITC-dextrans ($p > 0.05$) in spite of the difference in their molecular weights. The normalized permeability of FITC-ficoll 70 kDa was within the same permeability range of the linear dextrans ($p > 0.05$). In a previous study of the diffusion of macromolecules across sclera, a different trend between the permeability of globular proteins and linear dextrans was observed. Specifically, sclera was observed to be more permeable to BSA and IgG than dextrans in that study, presumably suggested to be a result of permeant-to-sclera "differential binding" in rabbit sclera.[18]

The effective pore sizes of the transport pathway across the sclera for the macromolecules were also investigated. Using Eqs. 5–7 and the permeability data of bevacizumab and ranibizumab, the average effective pore radius of the sclera was estimated to be 16 nm, which is within the same range as that determined previously.[19] This value is consistent with the effective pore size calculated using the permeability data of urea and the anti-VEGF proteins and is two times smaller than the pore size calculated using the urea and polysaccharide data. No reasonable pore size could be obtained from the permeability coefficient ratios of the dextrans, indicating that the dextran results of 20 to 150 kDa are not sensitive for the pore size estimation probably because of the flexible molecular structures of the polysaccharides.

Table 3 presents the transport lag times of the permeants across the sclera in the present study. Compared with the small hydrophilic molecules (log $D_{oct} < 0$) in a previous study,[22] the macromolecules demonstrated at least nine times longer lag times than the small molecules. The lag times of bevacizumab, ranibizumab, and FITC-BSA were longer than those of the dextrans and ficoll of comparable molecular weights ($p < 0.05$). Between the anti-VEGF drugs, bevacizumab with higher molecular weight showed a longer transport lag time than ranibizumab ($p < 0.05$).

Stability Study

The stability of bevacizumab and ranibizumab at 4°C and room temperature was examined by analyzing their anti-VEGF activities using ELISA over a period of 2 weeks. No significant changes in drug activities in the samples stored under both conditions as compared with the original stock solutions were observed ($p > 0.05$). In addition, the bevacizumab and ranibizumab solutions were clear during the time in the stability study as well as in the uptake and transport experiments. These results suggest that bevacizumab and ranibizumab were relatively stable over the duration of the uptake and transport experiments in the present study.

DISCUSSION

Transscleral Delivery of Bevacizumab and Ranibizumab

The sclera is believed to be a porous membrane that transscleral transport involves the mechanism of permeant partitioning into the pores of the sclera and diffusion in the pores across the membrane. For hydrophilic macromolecules, the molecular sizes of the macromolecules can be a dominant factor that affects their uptake and transport across the sclera. Size-exclusion effect can play an important role that limits the partitioning of anti-VEGF drugs into the sclera and their permeation across the membrane. Previous studies have shown that scleral permeability generally decreases with an increase in the molecular weight of a macromolecule.[18,19,30] In the present transport study, a similar trend was observed, and hindered transport is believed to be responsible for the low permeability

coefficients and long transport lag times of the anti-VEGF drugs. Particularly, ranibizumab demonstrated higher permeability and shorter transport lag time than bevacizumab. This is attributed to the lower molecular weight, higher diffusion coefficient, and less transport hindrance of ranibizumab than bevacizumab in transscleral permeation. Using the hindered transport theory and the transport data in the section *Transport Study*, these results suggest a transscleral transport pathway consisting of 16-nm radius effective pores. In the present uptake study, if the average effective pore radius of the sclera is 16 nm, the overall partition coefficients of the macromolecules would be ~1.7–5 times lower than those of small hydrophilic molecules (e.g., molecular weight of 60–270 Da) due to the steric hindrance of partitioning (size-exclusion effect) to the sclera according to the hindered transport theory. This is in general agreement with the differences between the partition coefficients of the macromolecules in the present study and those of the small hydrophilic molecules (log D_{oct} < 0) in a previous study[22] (~1.3–4 times). On the contrary, using the same effective pore radius (16 nm) and calculation, the partition coefficient of ranibizumab would be approximately 50% larger than that of bevacizumab. However, no significant difference was observed between the partition coefficients of bevacizumab and ranibizumab, possibly due to the variability of the uptake data. It is possible that the partitioning method in the present study was not sensitive enough for the pore size analysis.

Besides molecular weight, the molecular charge of a macromolecule can affect its uptake into and permeation across the sclera. At physiological pH of 7.4, human sclera is negatively charged.[31] Bevacizumab and ranibizumab were also net negatively charged at physiological pH.[32] As a result, charge–charge interactions may exist between the permeants and the sclera, and possible electrostatic repulsion between the anti-VEGF drugs and sclera should not be excluded. Permeant adsorption and binding to the sclera, for example, the collagen in the sclera, can also affect scleral uptake and transscleral permeation. For example, the transport lag times of bevacizumab, ranibizumab, and FITC-BSA were longer than those predicted from Eq. 8 using the permeability data, which may be due to permeant binding to sclera. The concentration-dependent uptake relationship of FITC-BSA also implies permeant-to-tissue binding. However, no specific concentration dependency was found with bevacizumab and ranibizumab in the uptake experiments. Another possible explanation of the observed uptake behavior of FITC-BSA is an increase in self-association of FITC-BSA with increasing concentration in the equilibration solution, leading to a decrease in the partition coefficient due to size exclusion of the aggregated FITC-BSA in the sclera. Further investigation on possible binding of anti-VEGF drugs and proteins to sclera is warranted.

Influence of Molecular Structure in Transscleral Delivery

The molecular structures (or particularly molecular shapes) of permeants were observed to influence transscleral transport of macromolecules. This important factor leads to the different transscleral transport behaviors of proteins and polysaccharides observed in the present study. The larger hydrodynamic radii of dextrans and ficoll than those of the globular proteins of comparable molecular weights (Table 1) suggest that the polysaccharides have more flexible structures than the proteins. The higher normalized permeability coefficients of dextrans in the transport study than those of the anti-VEGF proteins (Fig. 5) could also be explained by the more flexible structures of dextrans. With linear and flexible structures, dextrans could diffuse through the sclera pores in an orientation that represents smaller effective molecular radii than their hydrodynamic radii. Bevacizumab and ranibizumab have relatively solid and compact structures, which are less likely to change shapes during the permeation process. As a result, although the measured hydrodynamic radii of dextrans were larger than those of the proteins, dextrans exhibited considerable higher permeability than proteins in transscleral transport. Similarly, the higher normalized permeability coefficient of ficoll than BSA indicates that although ficoll is less

flexible than the linear dextrans, ficoll still demonstrates some degree of deformation relative to compact globular proteins such as BSA when permeating the sclera pores.

Molecular structures can also affect the transport lag time of macromolecules in transscleral delivery. As shown in Table 3, the polysaccharides tended to exhibit shorter lag times than the proteins of comparable molecular weights in transscleral transport. One possible interpretation could be the higher effective diffusion coefficients of dextrans in the pores of the sclera because of their relatively flexible structures, resulting in the shorter time for the polysaccharides to reach steady state in the experiments.

The different transport behaviors of proteins and polysaccharides across porous membranes of pore dimensions comparable to the macromolecules have been noted in previous studies. For example, dextrans and ficolls were shown to be more permeable across the glomerular capillary wall than proteins of similar Stokes–Einstein radii because the polysaccharides were more deformable than the globular proteins.[25,33] Asgeirsson et al.[34] found that the degree of polysaccharide glomerular “hyperpermeability” was proportional to the degree of “molecular extension” of the polysaccharides. Bohrer et al.[35] found that dextran could diffuse more readily than ficoll through synthetic microporous membranes when compared at similar Stokes–Einstein radii and suggested that this was due to the greater deformability of dextran than ficoll. However, such differences in transport behaviors between the flexible polysaccharides and rigid proteins have not been investigated in transscleral delivery.

On the basis of the findings in the present study, in addition to the influences from permeant molecular weight and possible permeant binding to membrane, the molecular structure and conformation of a permeant could play a major role in transscleral permeation of macromolecules. When studying transscleral permeation of proteins using polysaccharides, one should be aware that polysaccharides such as dextrans and ficolls may not be appropriate probes for transscleral permeation of therapeutic proteins because of their flexible structures.

Significance and Possible Implications of Transscleral Delivery Study of Bevacizumab and Ranibizumab

Anti-VEGF drugs such as bevacizumab and ranibizumab are widely used in the treatment of neovascular eye diseases, but the delivery of these macromolecular drugs to the posterior segment of the eye remains a challenge. Transscleral drug delivery could be a safe and effective drug delivery method. Only a few studies have investigated the transscleral permeation of bevacizumab and ranibizumab. Pescina et al.[36] investigated transscleral delivery of FITC-labeled bevacizumab using iontophoresis and found that anodal iontophoresis was able to significantly enhance the transport of the macromolecule across human sclera. Chopra et al.[19] studied the passive and iontophoretic transport of bevacizumab across human sclera and demonstrated the feasibility of enhancing bevacizumab transport using iontophoresis. Singh et al.[37] explored the delivery of ranibizumab by macroesis using rabbit sclera. However, the transport mechanisms of macromolecules across the sclera and its barrier properties have not been systematically studied. There has been no direct comparison of transscleral transport of bevacizumab and ranibizumab in human sclera, and the partitioning and loading capacity of the tissue for these macromolecules are not well understood. The present study investigated the uptake and transport behaviors of anti-VEGF drugs bevacizumab and ranibizumab using human sclera. The higher transscleral permeation of ranibizumab than bevacizumab and the shorter transport lag time of ranibizumab than bevacizumab suggest that ranibizumab could be more effectively delivered through the transscleral route, for example, in subconjunctival injection or episcleral implant. However, the smaller molecular size of ranibizumab does not provide

a significant advantage in sclera loading that could serve as a drug reservoir in transscleral delivery compared with bevacizumab.

The data obtained in the present study provide insights into the uptake and transport properties of human sclera for transscleral delivery of bevacizumab and ranibizumab. These data are important in the development of transscleral delivery systems for the delivery of anti-VEGF drugs to the posterior segment of the eye. For example, assuming no ocular clearance, with the permeability coefficient of 9.9×10^{-7} cm/s for ranibizumab, a drug donor of 10 mg/mL will deliver approximately 0.9 mg of the drug across 1 cm^2 sclera in transscleral delivery of 1 day. This amount is larger than the amount of ranibizumab administered monthly via intravitreal injection in current neovascular disease therapy (0.5 mg). If the sclera is the main barrier in transscleral delivery, ocular delivery systems and devices such as sustained-release formulations and episcleral implants may provide effective transscleral delivery of anti-VEGF drugs to the posterior eye. However, the sclera is not the only barrier involved in transscleral delivery. Other barriers such as the retinal pigment epithelium and conjunctiva should also be considered in practice. Dynamic barriers such as choroidal blood flow and orbital clearance should be taken into account when extrapolating the present *in vitro* results to *in vivo* conditions.

CONCLUSIONS

The present study investigated the transport and uptake behaviors of human sclera for anti-VEGF drugs bevacizumab and ranibizumab and characterized the sclera barrier properties such as the effects of molecular structures of the macromolecules upon transscleral permeation. Because of the molecular sizes of bevacizumab and ranibizumab, these macromolecules exhibited low partition coefficients, low permeability coefficients, as well as long transport lag times in the present uptake and transport studies with human sclera. Hindered transport played an important role in transscleral transport and led to the lower permeabilities of bevacizumab and ranibizumab than expected according to their diffusion coefficients. The present study also provides insights into the influence of molecular structures on transscleral transport behaviors of the macromolecules. Polysaccharides such as dextrans and ficoll with flexible structures were observed to have higher permeability coefficients and shorter transport lag times than those of compact proteins of comparable molecular weights. Thus, consideration should be given to the suitability of using polysaccharides as surrogates to study transscleral delivery of proteins. As dextrans are frequently used as molecular probes to study the permeability of membranes to biological macromolecules such as transscleral permeability of proteins, the effects of molecular structures (shapes) should not be overlooked in these studies.

Acknowledgments

The research was supported by National Institutes of Health (NIH) grant number EY 015181. The authors acknowledge the use of tissues procured by the NDRI with the support from NIH grant number 5 U42 RR006042. The authors thank Dr. Paul Bernstein and Moran Eye Center at the University of Utah for kindly supplying some of the sclera tissues used in this study. The authors thank Dr. Robert Hutchins and Dr. Stewart Krug for supplying the Lucentis used in this study, and Poonam Chopra for her help in developing the ELISA assay method.

REFERENCES

1. Resnikoff S, Pascolini D, Etya'ale D, Kocur I, Pararajasegaram R, Pokharel GP, Mariotti SP. Global data on visual impairment in the year 2002. Bull World Health Organ. 2004; 82(11):844–851. [PubMed: 15640920]

2. Friedman DS, O'Colmain BJ, Muñoz B, Tomany SC, McCarty C, de Jong PT, Nemesure B, Mitchell P, Kempen J. Eye Diseases Prevalence Research Group. Prevalence of age-related macular degeneration in the United States. Arch Ophthalmol. 2004; 122(4):564–572. [PubMed: 15078675]
3. Congdon N, O'Colmain B, Klaver CC, Klein R, Muñoz B, Friedman DS, Kempen J, Taylor HR, Mitchell P. Eye Diseases Prevalence Research Group. Causes and prevalence of visual impairment among adults in the United States. Arch Ophthalmol. 2004; 122(4):477–485. [PubMed: 15078664]
4. Penn JS, Madan A, Caldwell RB, Bartoli M, Caldwell RW, Hartnett ME. Vascular endothelial growth factor in eye disease. Prog Retin Eye Res. 2008; 27(4):331–371. [PubMed: 18653375]
5. Jager RD, Mieler WF, Miller JW. Age-related macular degeneration. N Engl J Med. 2008; 358(24): 2606–2617. [PubMed: 18550876]
6. Simó R, Hernández C. Intravitreous anti-VEGF for diabetic retinopathy: Hopes and fears for a new therapeutic strategy. Diabetologia. 2008; 51(9):1574–1580. [PubMed: 18404258]
7. Ciulla TA, Rosenfeld PJ. Anti-vascular endothelial growth factor therapy for neovascular ocular diseases other than age-related macular degeneration. Curr Opin Ophthalmol. 2009; 20(3):166–174. [PubMed: 19381089]
8. Kinnunen K, Ylä-Herttuala S. Vascular endothelial growth factors in retinal and choroidal neovascular diseases. Ann Med. 2012; 44:1–17. [PubMed: 21284527]
9. Lynch SS, Cheng CM. Bevacizumab for neovascular ocular diseases. Ann Pharmacother. 2007; 41(4):614–625. [PubMed: 17355998]
10. Rosenfeld PJ, Brown DM, Heier JS, Boyer DS, Kaiser PK, Chung CY, Kim RY. MARINA Study Group. Ranibizumab for neovascular age-related macular degeneration. N Engl J Med. 2006; 355(14):1419–1431. [PubMed: 17021318]
11. Kourlas H, Abrams P. Ranibizumab for the treatment of neovascular age-related macular degeneration: A review. Clin Ther. 2007; 29(9):1850–1861. [PubMed: 18035187]
12. Gunther JB, Altaweel MM. Bevacizumab (Avastin) for the treatment of ocular disease. Surv Ophthalmol. 2009; 54(3):372–400. [PubMed: 19422965]
13. Hernandez-Pastor LJ, Ortega A, Garcia-Layana A, Giraldez J. Ranibizumab for neovascular age-related macular degeneration. Am J Health Syst Pharm. 2008; 65(19):1805–1814. [PubMed: 18796421]
14. Frenkel RE, Haji SA, La M, Frenkel MP, Reyes A. A protocol for the retina surgeon's safe initial intravitreal injections. Clin Ophthalmol. 2010; 4:1279–1285. [PubMed: 21139676]
15. Olsen TW, Aaberg SY, Geroski DH, Edelhauser HF. Human sclera: Thickness and surface area. Am J Ophthalmol. 1998; 125(2):237–241. [PubMed: 9467451]
16. Geroski DH, Edelhauser HF. Transscleral drug delivery for posterior segment disease. Adv Drug Deliv Rev. 2001; 52(1):37–48. [PubMed: 11672874]
17. Olsen TW, Edelhauser HF, Lim JI, Geroski DH. Human scleral permeability. Effects of age, cryotherapy, transscleral diode laser, and surgical thinning. Invest Ophthalmol Vis Sci. 1995; 36(9):1893–1903. [PubMed: 7543465]
18. Ambati J, Canakis CS, Miller JW, Gragoudas ES, Edwards A, Weissgold DJ, Kim I, Delori FC, Adamis AP. Diffusion of high molecular weight compounds through sclera. Invest Ophthalmol Vis Sci. 2000; 41(5):1181–1185. [PubMed: 10752958]
19. Chopra P, Hao J, Li SK. Iontophoretic transport of charged macromolecules across human sclera. Int J Pharm. 2010; 388(1–2):107–113. [PubMed: 20045044]
20. Ambati J, Gragoudas ES, Miller JW, You TT, Miyamoto K, Delori FC, Adamis AP. Transscleral delivery of bioactive protein to the choroid and retina. Invest Ophthalmol Vis Sci. 2000; 41(5): 1186–1191. [PubMed: 10752959]
21. Demetriades AM, Deering T, Liu H, Lu L, Gehlbach P, Packer JD, Mac Gabhann F, Popel AS, Wei LL, Campochiaro PA. Trans-scleral delivery of antiangiogenic proteins. J Ocul Pharmacol Ther. 2008; 24(1):70–79. [PubMed: 18370877]
22. Wen H, Hao J, Li SK. Influence of permeant lipophilicity on permeation across human sclera. Pharm Res. 2010; 27(11):2446–2456. [PubMed: 20734114]
23. Peck KD, Ghanem AH, Higuchi WI. Hindered diffusion of polar molecules through and effective pore radii estimates of intact and ethanol treated human epidermal membrane. Pharm Res. 1994; 11(9):1306–1314. [PubMed: 7816761]

24. Deen WM. Hindered transport of large molecules in liquid-filled pores. AIChE J. 1987; 33:1409–1425.
25. Venturoli D, Rippe B. Ficoll and dextran vs. globular proteins as probes for testing glomerular permselectivity: Effects of molecular size, shape, charge, and deformability. Am J Physiol Renal Physiol. 2005; 288(4):F605–F613. [PubMed: 15753324]
26. Böhme U, Scheler U. Effective charge of bovine serum albumin determined by electrophoresis NMR. Chem Phys Lett. 2007; 435(4–6):342–345.
27. Squire PG, Moser P, O'Konski CT. The hydrodynamic properties of bovine serum albumin monomer and dimer. Biochemistry. 1968; 7(12):4261–4272. [PubMed: 5750167]
28. Wen J, Arakawa T, Philo JS. Size-exclusion chromatography with on-line light-scattering, absorbance, and refractive index detectors for studying proteins and their interactions. Anal Biochem. 1996; 240(2):155–166. [PubMed: 8811899]
29. Beck RE, Schultz JS. Hindrance of solute diffusion within membranes as measured with microporous membranes of known pore geometry. Biochim Biophys Acta. 1972; 255(1):273–303. [PubMed: 4334681]
30. Nicoli S, Ferrari G, Quarta M, Macaluso C, Santi P. *In vitro* transscleral iontophoresis of high molecular weight neutral compounds. Eur J Pharm Sci. 2009; 36(4–5):486–492. [PubMed: 19110056]
31. Li SK, Zhang Y, Zhu H, Higuchi WI, White HS. Influence of asymmetric donor-receiver ion concentration upon transscleral iontophoretic transport. J Pharm Sci. 2005; 94(4):847–860. [PubMed: 15736190]
32. Li SK, Liddell MR, Wen H. Effective electrophoretic mobilities and charges of anti-VEGF proteins determined by capillary zone electrophoresis. J Pharm Biomed Anal. 2011; 55(3):603–607. [PubMed: 21269789]
33. Rennke HG, Venkatachalam MA. Glomerular permeability of macromolecules. Effect of molecular configuration on the fractional clearance of uncharged dextran and neutral horseradish peroxidase in the rat. J Clin Invest. 1979; 63(4):713–717. [PubMed: 438331]
34. Asgeirsson D, Venturoli D, Fries E, Rippe B, Rippe C. Glomerular sieving of three neutral polysaccharides, polyethylene oxide and bikunin in rat. Effects of molecular size and conformation. Acta Physiol (Oxf). 2007; 191(3):237–246. [PubMed: 17935524]
35. Bohrer MP, Patterson GD, Carroll PJ. Hindered diffusion of dextran and ficoll in microporous membranes. Macromolecules. 1984; 17:1170–1173.
36. Pescina S, Ferrari G, Govoni P, Macaluso C, Padula C, Santi P, Nicoli S. *In-vitro* permeation of bevacizumab through human sclera: Effect of iontophoresis application. J Pharm Pharmacol. 2010; 62(9):1189–1194. [PubMed: 20796199]
37. Singh RP, Mathews ME, Kaufman M, Riga A. Transcleral delivery of triamcinolone acetonide and ranibizumab to retinal tissues using macroesis. Br J Ophthalmol. 2010; 94(2):170–173. [PubMed: 20139290]

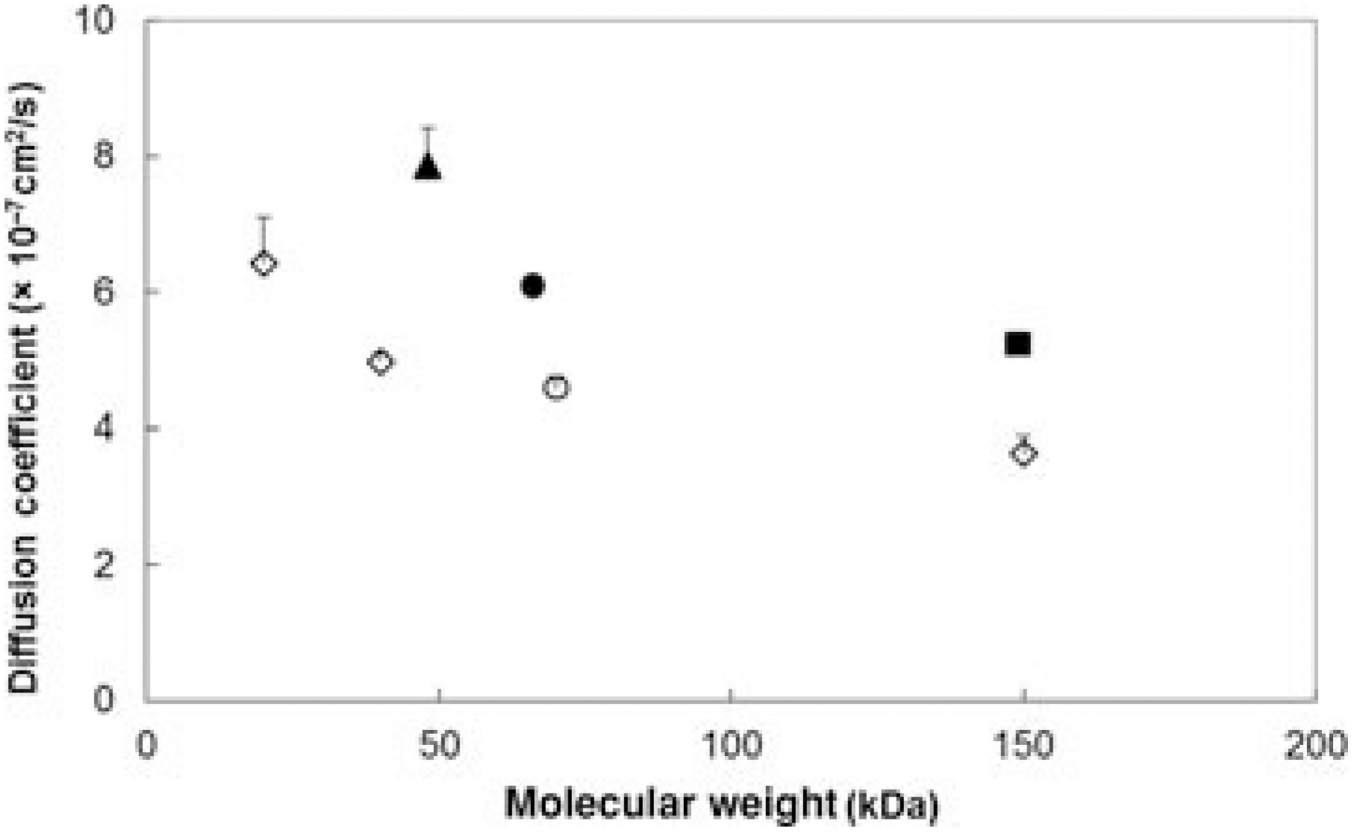

Figure 1.

Relationship between aqueous diffusion coefficients at 37°C and molecular weights of the permeants. Diffusion coefficients were calculated by $D=\frac{k_B T}{6\pi\eta r}$, where k_B is the Boltzmann constant, T is the absolute temperature, η is the viscosity of water at 37°C, and r is the average hydrodynamic radius of the permeant at 25°C assuming the radius does not change with temperature. Symbols: closed square, bevacizumab; closed triangle, ranibizumab; closed circle, FITC-BSA; open circle, FITC-ficoll 70 kDa; open diamonds, FITC-dextrans 20, 40, and 150 kDa. Data represent the mean and standard deviation for each permeant.

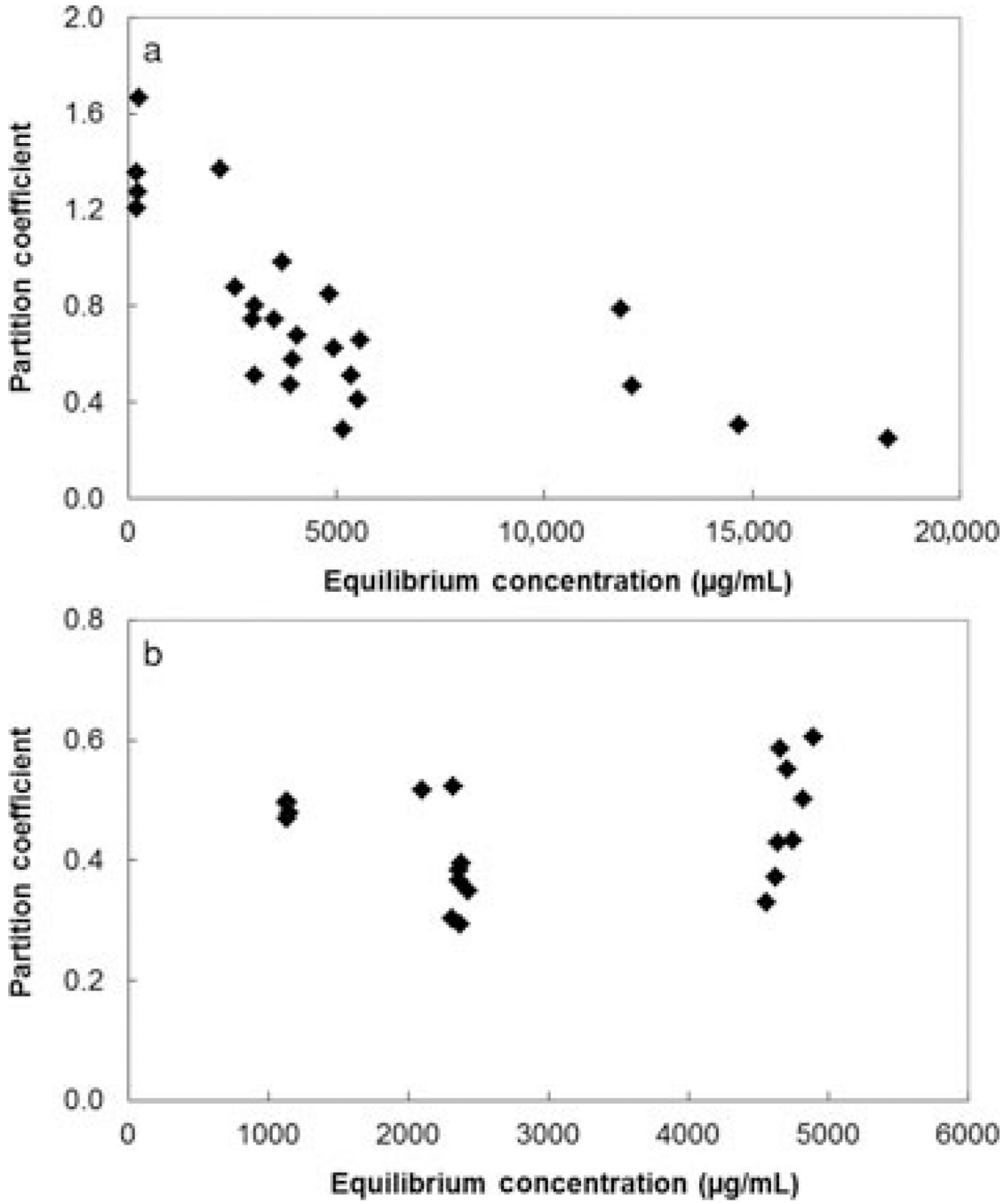

Figure 2.
Plots of partition coefficients of (a) FITC-BSA and (b) FITC-dextran 150 kDa to human sclera versus equilibrium concentrations. Each data point represents the result of a single experiment for the permeant.

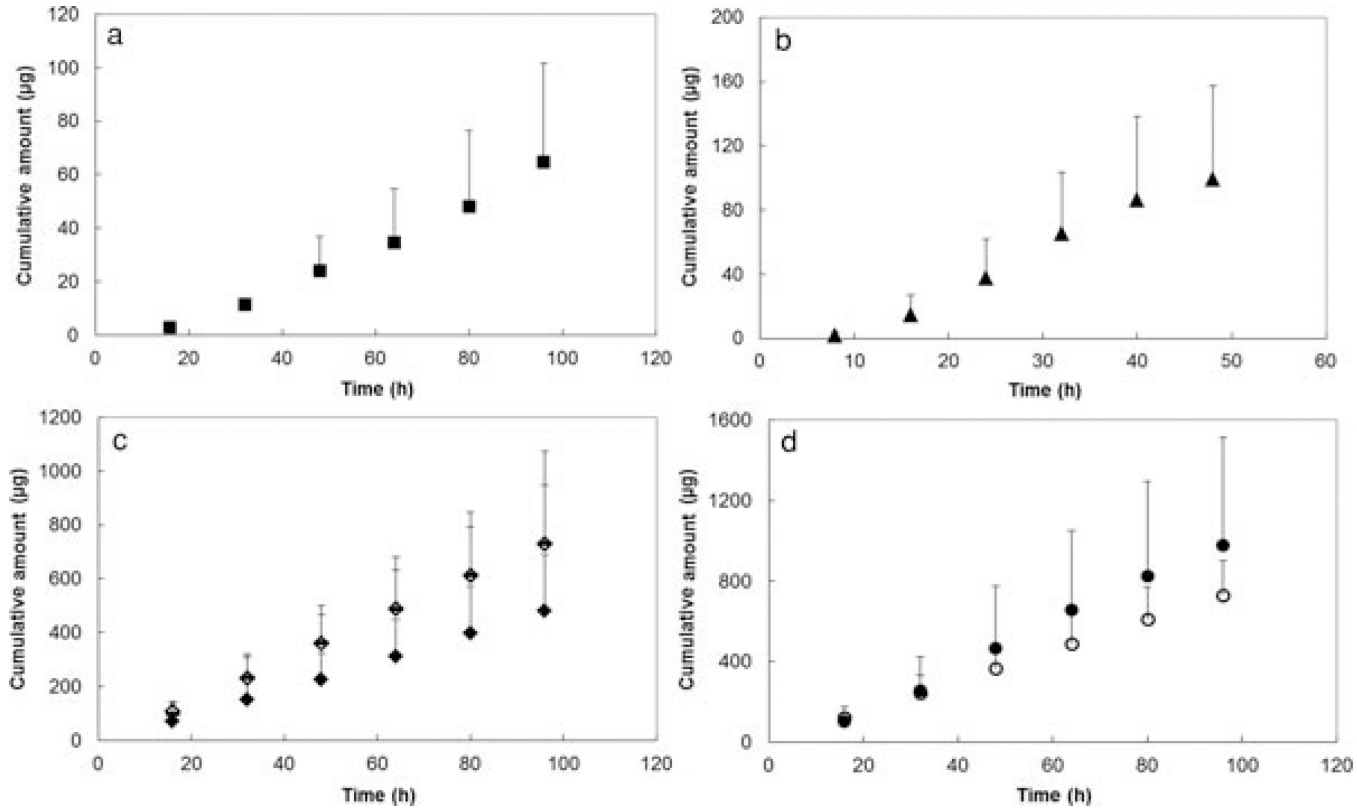

Figure 3.

Plots of cumulative amounts of (a) bevacizumab; (b) ranibizumab; (c) FITC-dextrans 20, 40, and 150 kDa; and (d) FITC-BSA and FITC-ficoll 70 kDa permeated across human sclera versus time. Symbols: closed squares, bevacizumab; closed triangles, ranibizumab; solid lines, FITC-dextran 20 kDa; open diamonds, FITC-dextran 40 kDa; closed diamonds, FITC-dextran 150 kDa; closed circles, FITC-BSA; open circles, FITC-ficoll 70 kDa. Data represent the mean and standard deviation of at least three sclera samples for each permeant.

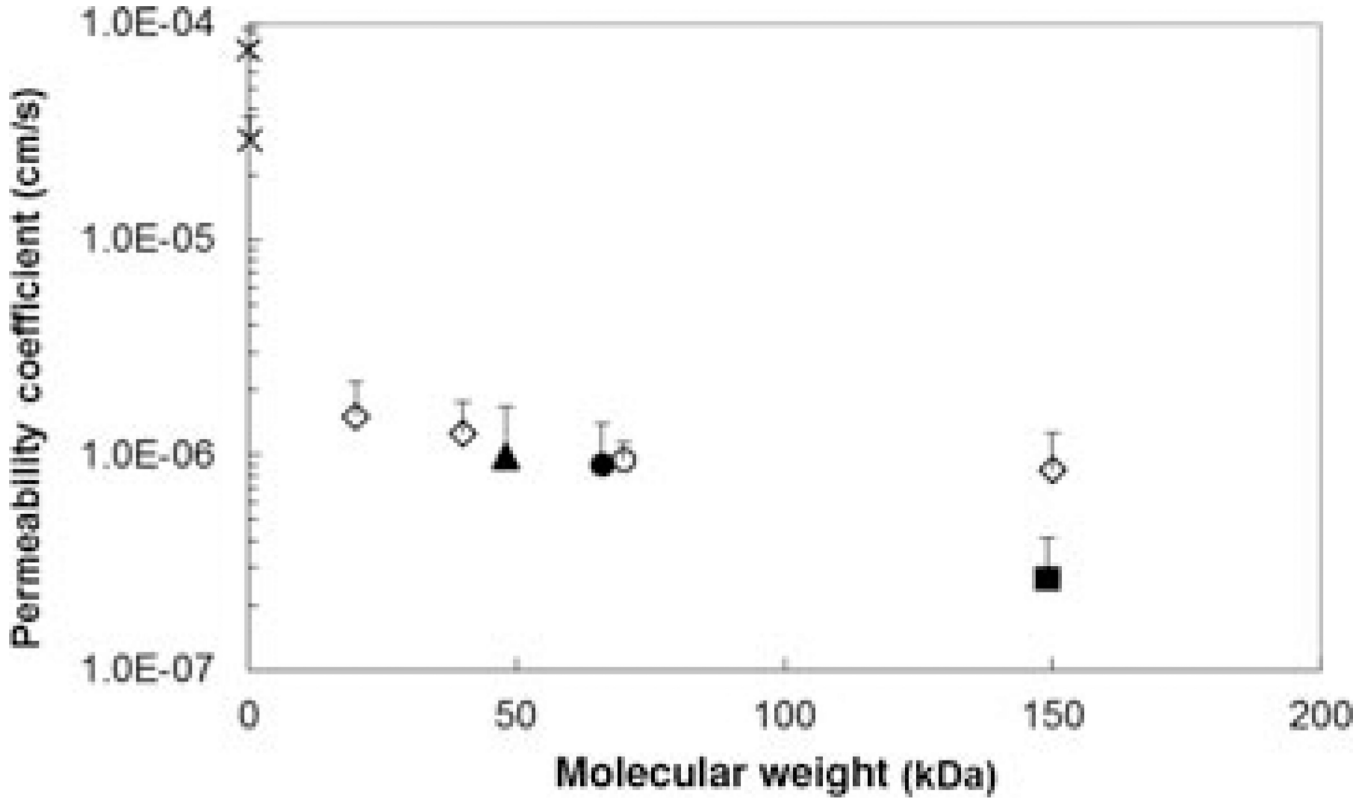

Figure 4.

Relationship between the steady-state permeability coefficients and molecular weights of permeants in the human sclera transport experiment. The permeability coefficient data of urea and atenolol are obtained from a previous study.[22] Symbols: closed square, bevacizumab; closed triangle, ranibizumab; closed circle, FITC-BSA; open circle, FITC-ficoll 70 kDa; open diamonds, FITC-dextrans 20, 40, and 150 kDa; crosses, urea and atenolol. Data represent the mean and standard deviation of at least three sclera samples for each permeant.

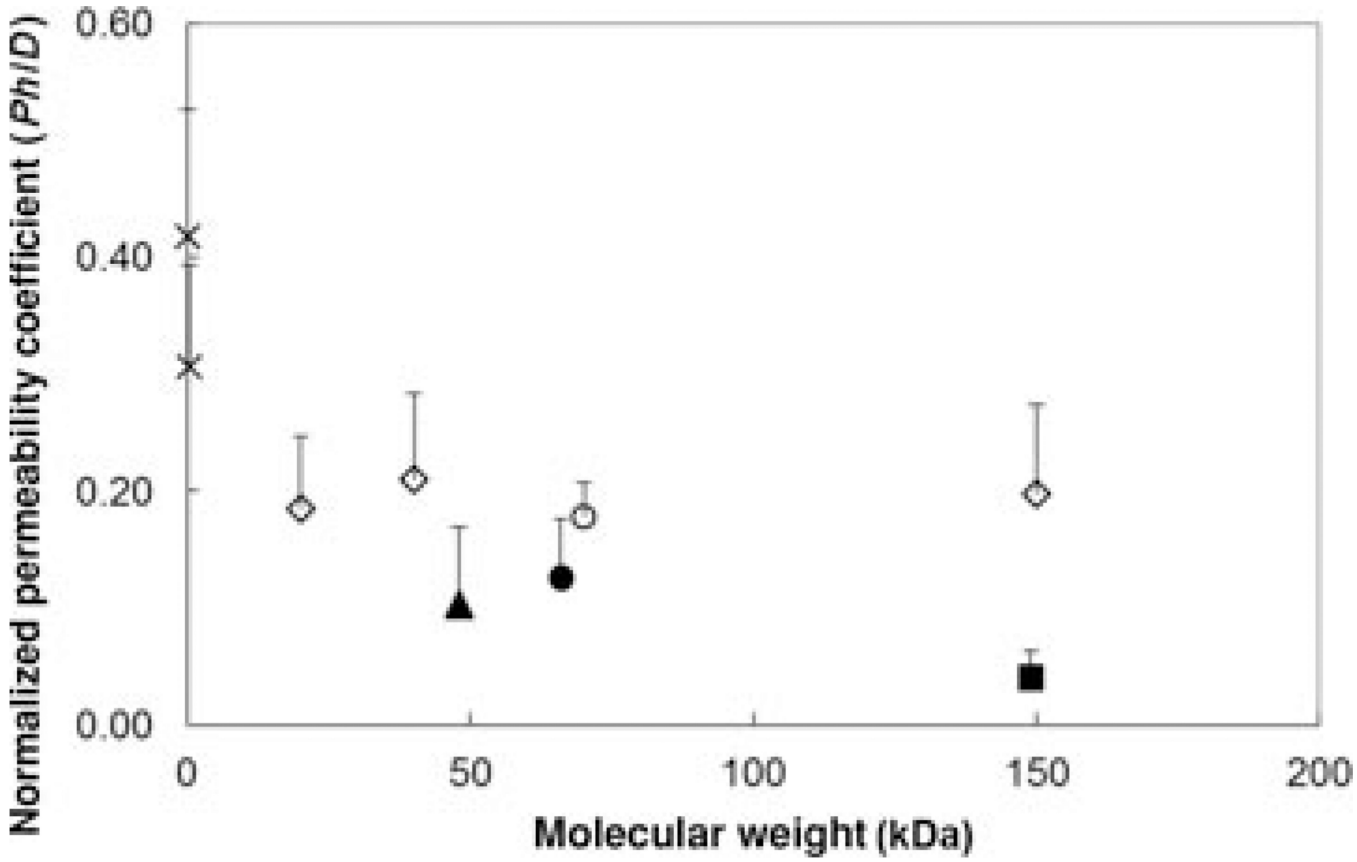

Figure 5.

Relationship between normalized permeability coefficients (*Ph/D*) of human sclera and molecular weights of the permeants. The normalized permeability coefficients were calculated by multiplying the steady-state permeability coefficients (*P*) to sclera thicknesses (*h*) and then divided by the free aqueous diffusion coefficients (*D*) of the permeants. The normalized permeability coefficients are related to the hindrance factors according to Eq. 4. The permeability coefficient data of urea and atenolol are obtained from a previous study[22] and their diffusion coefficients were calculated using Stokes–Einstein equation with the correction according to Beck and Schultz.[29] Symbols: closed square, bevacizumab; closed triangle, ranibizumab; closed circle, FITC-BSA; open circle, FITC-ficoll 70 kDa; open diamonds, FITC-dextrans 20, 40, and 150 kDa; crosses, urea and atenolol. Data represent the mean and standard deviation of at least three sclera samples for each permeant.

Table 1

Molecular Weights and Hydrodynamic Radii of the Permeants

	Molecular Weight (kDa)	Hydrodynamic Radius[a] (nm)
Bevacizumab	149	6.3 ± 0.1
Ranibizumab	48	4.2 ± 0.3
FITC-BSA	66	5.4 ± 0.1
FITC-ficoll 70 kDa	70	7.2 ± 0.3
FITC-dextran 20 kDa	20	5.2 ± 0.5
FITC-dextran 40 kDa	40	6.6 ± 0.2
FITC-dextran 150 kDa	150	9.0 ± 0.6

[a]The hydrodynamic radius was measured using dynamic light scattering at 25°C. Data represent the mean and standard deviation from at least five measurements.

Table 2

Scleral Partition Coefficients for the Permeants

	Mean ± SD[a]	Range
Bevacizumab	0.31 ± 0.14	0.08–0.49
Ranibizumab	0.31 ± 0.10	0.10–0.43
FITC-BSA[b]		0.25–1.67
FITC-ficoll 70 kDa	0.39 ± 0.05	0.32–0.43
FITC-dextran 20 kDa	0.34 ± 0.08	0.28–0.45
FITC-dextran 40 kDa	0.32 ± 0.06	0.27–0.41
FITC-dextran 150 kDa	0.44 ± 0.09	0.29–0.61

[a] Data represent the mean and standard deviation of at least four sclera samples for each permeant.

[b] Concentration-dependent uptake was observed for FITC-BSA, and the mean value was not calculated.

Table 3

Transport Lag Times of Permeants*

	Lag Time (h)
Bevacizumab	24 ± 13
Ranibizumab	10 ± 2
FITC-BSA	9.2 ± 6.2
FITC-ficoll 70 kDa	5.0 ± 3.8
FITC-dextran 20 kDa	2.7 ± 1.0
FITC-dextran 40 kDa	2.7 ± 1.0
FITC-dextran 150 kDa	4.4 ± 2.8

* Data represent the mean and standard deviation of at least three sclera samples for each permeant.